Original Article

A convenient and reproducible protocol for acquisition of the hepatocyte phase for liver function-impaired patients in gadoxetic acid disodium-enhanced magnetic resonance imaging

Chao Wang[1#^], Wei-Rong Sun[2#], Ning Wu[2^], Zhuang Zhang[1^], Lai-Xing Zhang[1^], Wan-Qing Yi[1], Xiao-Dong Yuan[2^]

[1]Department of Graduate, Hebei North University, Zhangjiakou, China; [2]Department of Radiology, the 8th Medical Center of Chinese PLA General Hospital, Beijing, China

Contributions: (I) Conception and design: C Wang, XD Yuan; (II) Administrative support: XD Yuan, WR Sun; (III) Provision of study materials or patients: C Wang, WR Sun, XD Yuan; (IV) Collection and assembly of data: C Wang, WR Sun, N Wu; (V) Data analysis and interpretation: All authors; (VI) Manuscript writing: All authors; (VII) Final approval of manuscript: All authors.

[#]These authors contributed equally to this work as co-first authors.

Correspondence to: Xiao-Dong Yuan, MD, PhD. Department of Radiology, the 8th Medical Center of Chinese PLA General Hospital, 17 Heishanhu Rd., Haidian District, Beijing 100091, China. Email: yuanxiaodongzj@163.com.

Background: The hepatocyte phase (HCP) in gadoxetic acid disodium (Gd-EOB-DTPA)-enhanced magnetic resonance imaging (MRI) plays an important role in the detection and characterization of liver lesions, treatment planning, and liver function evaluation. However, the imaging protocol is complicated and time-consuming. This cross-sectional study aimed to develop a convenient and reproducible protocol for the HCP acquisition in Gd-EOB-DTPA-enhanced MRI.

Methods: A total of 107 patients were prospectively included and assigned to three groups based on Child-Pugh (CP) classification, with 37, 40, and 30 in the non-cirrhosis, CP A, and CP B groups, respectively. Dynamic HCPs were acquired every 5 min after the Gd-EOB-DTPA administration and ended in 25 min in non-cirrhosis patients and 40 min in cirrhotic patients. The HCP acquired 5 min after the initial visualization of the intrahepatic bile duct (IBD) was selected from the dynamic HCPs as the adequate HCP ($HCP_{proposed}$) and the corresponding acquisition time was recorded as $Time_{proposed}$. In addition, according to the 2016 Expert Consensus (EC) on the definition of the adequate HCP from the European Society of Gastrointestinal and Abdominal Radiology (ESGAR), the adequate HCP_{EC} and the corresponding $Time_{EC}$ were also determined from the dynamic HCPs. The hepatic relative enhancement ratio (RER), the contrast-to-noise ratio (CNR), and signal-to-noise ratio (SNR) of hepatic focal lesions in the HCP_{EC} and $HCP_{proposed}$ images, as well as the $Time_{EC}$ and $Time_{proposed}$ were compared by the paired *t*-test for the three groups, respectively. Inter-observer agreement of the determination of the HCP_{EC} and $HCP_{proposed}$ was compared by the χ^2 test.

Results: The RER, CNR, and SNR showed no significant difference between the HCP_{EC} and $HCP_{proposed}$ in all three groups (all P>0.05). The paired differences between $Time_{EC}$ and $Time_{proposed}$ were 1.08±3.56 min (P=0.07), 2.88±4.22 min (P<0.001), and 5.83±5.27 min (P<0.001) in the three groups, respectively. Inter-observer agreement of the determination of the HCP_{EC} and $HCP_{proposed}$ were 0.804 (86/107) and 0.962 (103/107), respectively (χ^2=13.09, P=0.001).

^ ORCID: Chao Wang, 0000-0003-3446-9045; Ning Wu, 0000-0002-9307-3115; Zhuang Zhang, 0000-0002-9270-8342; Lai-Xing Zhang, 0000-0001-7034-8043; Xiao-Dong Yuan, 0000-0003-1964-5098.

© Quantitative Imaging in Medicine and Surgery. All rights reserved.

Conclusions: The adequate HCP could be acquired 5 min after the initial visualization of the IBD, which could serve as a convenient and reproducible protocol for the HCP imaging.

Keywords: Gadoxetic acid disodium (Gd-EOB-DTPA); magnetic resonance imaging (MRI); hepatocyte phase (HCP); intrahepatic bile duct (IBD)

Submitted Aug 13, 2023. Accepted for publication Dec 11, 2023. Published online Jan 18, 2024.
doi: 10.21037/qims-23-1147
View this article at: https://dx.doi.org/10.21037/qims-23-1147

Introduction

Gadoxetic acid disodium (Gd-EOB-DTPA) is a dual-channel, specifically, hepatic and renal excretory, magnetic resonance imaging (MRI) contrast agent. It is rapidly dispersed into the blood circulation after intravenous administration enabling dynamic contrast enhancement (DCE) MRI of the liver, then undergoes specific uptake into liver cells by organic anion transporting polypeptides 1B1/1B3 (OATP1B1/1B3) on the hepatocyte membrane producing [hepatocyte phase (HCP)] MRI of the liver (1). Gd-EOB-DTPA-enhanced MRI is extensively used for hepatic focal lesion detection and characterization as well as efficacy monitoring and liver function evaluation (2-6). Sufficient drug accumulation in the liver is a prerequisite for obtaining the HCP image with adequate liver enhancement, namely, the adequate HCP. The uptake speed of Gd-EOB-DTPA by the hepatocytes varies substantially among patients because of individual differences in liver function (7). In most patients, drug accumulation in the liver peaks within 20 min, then is maintained at a relatively high plateau with concurrent gradual drug excretion from the bile. Therefore, at the early stage of its clinical practice, the HCP was generally acquired 20 min after intravenous administration (8).

Previous studies have demonstrated that the adequate HCP could be acquired as early as 10–15 min after the Gd-EOB-DTPA administration in patients with normal liver function (9-12). For patients with mild cirrhosis, it is possible to obtain the adequate HCP within 15–20 min after the administration, whereas in patients with severe liver dysfunction, a longer delay time is proposed for adequate HCP acquisition (12-14). Investigators proposed that a 20- or even 30-min delay for HCP acquisition may further improve liver enhancement and thus the contrast between liver parenchyma and intrahepatic lesions (13,15). Therefore, a personalized acquisition protocol for obtaining the adequate HCP in the shortest possible time is needed in clinical practice of the Gd-EOB-DTPA-enhanced MRI. However, setting the acquisition time of the adequate HCP according to the level of hepatic impairment requires advance assessment of laboratory indicators of liver function, which is of low practicality in clinical practice, especially for outpatients. The 2016 Expert Consensus (EC) of the European Society of Gastrointestinal and Abdominal Radiology (ESGAR) recommends that the HCP can be considered adequate when Gd-EOB-DTPA is detected in the intrahepatic bile ducts (IBDs) and the vessels are definitely hypointense in comparison to the background parenchyma of the liver (16). To follow the 2016 EC of the ESGAR, MRI signals of multiple structures, including IBD, liver parenchyma, and intrahepatic vessels should be continuously observed during the magnetic resonance (MR) scanning process, which increases labor intensity and the odds of misjudgment from the MR technicians. In addition, the judgement of the adequate HCP also takes time and might prolong the MRI examination. Based on the abovementioned reports and our clinical experience, we hypothesized that the adequate HCP could be acquired 5 min after the initial visualization of the IBD and validated it by comparing with the adequate HCP determined according to the 2016 EC of the ESGAR. We present this article in accordance with the STROBE reporting checklist (available at https://qims.amegroups.com/article/view/10.21037/qims-23-1147/rc).

Methods

Ethical considerations

The study was conducted in accordance with the Declaration of Helsinki (as revised in 2013). This prospective study was approved by the Ethics Committee of the 8th Medical Center of PLA General Hospital (30920200825701240), and written informed consent was provided by all patients.

© Quantitative Imaging in Medicine and Surgery. All rights reserved.

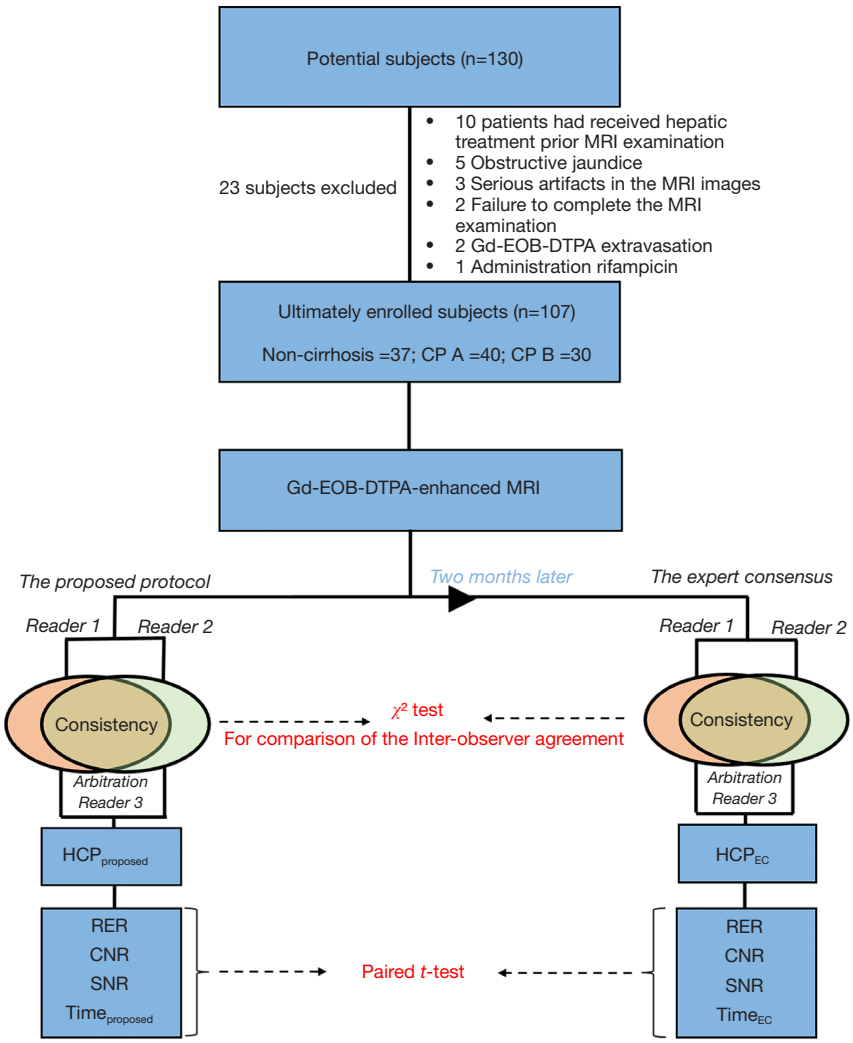

Figure 1 Study flowchart. MRI, magnetic resonance imaging; Gd-EOB-DTPA, gadoxetic acid disodium; CP, Child-Pugh; $HCP_{proposed}$, the HCP acquired 5 min after the initial visualization of the intrahepatic bile ducts; HCP_{EC}, adequate HCP determined upon the 2016 Expert Consensus of the European Society of Gastrointestinal and Abdominal Radiology; RER, relative enhancement ratio; CNR, contrast-to-noise ratio; SNR, signal-to-noise ratio; HCP, hepatocyte phase; EC, expert consensus.

Participants

The sample size of the study was determined by PASS (https://www.ncss.com/software/pass/). A total of 130 potential participants with liver diseases referred for Gd-EOB-DTPA-enhanced MRI examination between August 2020 and June 2022 were prospectively included (*Figure 1*), and Child-Pugh (CP) classification and estimated glomerular filtration rate (eGFR) for all patients were obtained 1 week before the MRI examination. Patients were selected for this study in accordance with the following criteria: (I) imaging findings of cirrhosis or occupying liver lesions within 2 weeks before the MRI examination; (II) no contraindications to MR scanning; (III) no history of allergy to Gd-EOB-DTPA; (IV) eGFR >30 mL/min/1.73 m^2. The exclusion criteria were as follows: (I) clinical treatment before Gd-EOB-DTPA-enhanced MRI; (II) imaging findings of biliary obstruction; (III) significant artifacts in Gd-EOB-DTPA-enhanced MRI; (IV) inability to cooperate during the MR scanning; (V) definite extravasation of the contrast agent during injection; (VI) treatment with rifampicin and/or erythromycin within three days before the examination; (VII) CP grade C of the liver function.

Patients were assigned to the non-cirrhosis, CP A, and

© Quantitative Imaging in Medicine and Surgery. All rights reserved.

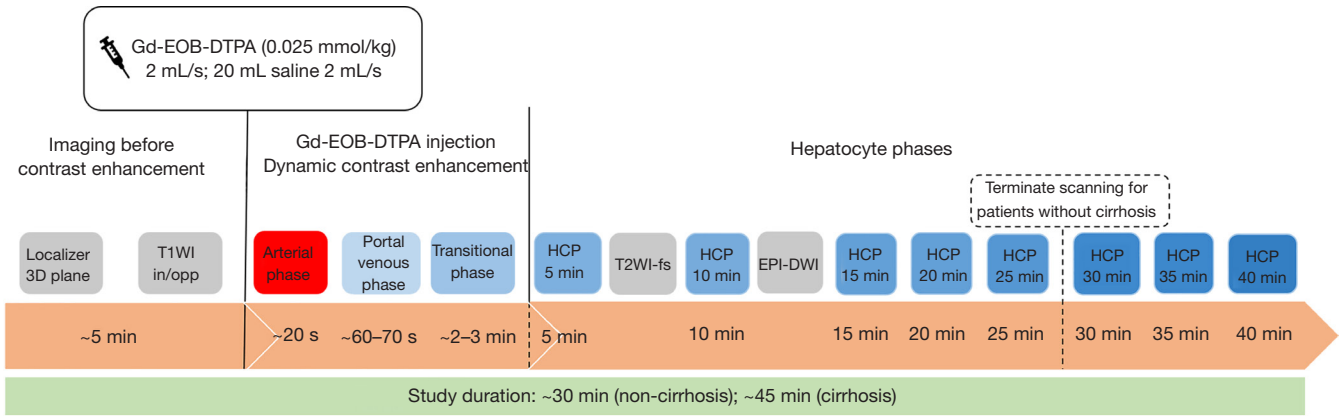

Figure 2 MRI scan flow. Gd-EOB-DTPA, gadoxetic acid disodium; T1WI, T1-weighted imaging; in/opp, in and opposite; HCP, hepatocyte phase; T2WI, T2-weighted imaging; FS, fat saturation; EPI, echo planar imaging; DWI, diffusion-weighted imaging.

CP B groups based on the CP classification system (17), and the patients with CP B grade had worse liver function than those with CP A grade. The study flowchart is shown in *Figure 1*. Non-cystic hepatic lesions with a diameter ≥1 cm were included in MRI signal analysis. In case of multiple eligible hepatic lesions, the largest lesion was analyzed. Liver cysts were not included in the analysis. The final diagnosis of a focal liver lesion was made by surgical or puncture histopathology or typical image features (18,19).

MRI scanning protocol

Gd-EOB-DTPA-enhanced MRI was performed on a 3.0T MRI scanner (Magnetom Skyra; Siemens Healthcare, Erlangen, Germany) with the use of a combination of body-spine array coil elements (18-channel body matrix coil and 32-channel spine matrix coil) for signal reception. Patients underwent 4-hour fasting and breath training prior to MRI examination. Prior to contrast medium administration, all patients were imaged with the following unenhanced sequences: Localizer 3-dimensional (3D) plane, T1-weighted imaging (T1WI) in and opposite (in/opp) phase. Each patient received the standard dose, 0.025 mmol/kg of body weight, of Gd-EOB-DTPA (Primovist; Bayer Schering Pharma, Berlin, Germany) as an intravenous bolus injection, which was administered at a rate of 2 mL/s by means of a power injector (Tennessee XD2003; Ulrich Medical, Baden-Wuerttemberg, Germany). The bolus injection was followed by a 20 mL saline flush at a rate of 2 mL/s. After administration, volumetric interpolated breath-hold examination (VIBE) T1-weighted fat-suppressed (FS) (Dixon) sequences were acquired in different phases: hepatic arterial (~20 s), portal venous (~60–70 s), transitional phases (~2–3 min), followed by the HCP serials. The HCP were acquired every 5 min after the Gd-EOB-DTPA administration, with 5 phases of acquisition for non-cirrhosis patients (end in 25 min) and 8 for cirrhotic patients (end in 40 min). The T2-weighted imaging (T2WI)-FS was acquired between 5-min HCP and 10-min HCP, and the echo-planar imaging diffusion-weighted imaging (EPI-DWI) was acquired between 10- and 15-min HCP (*Figure 2*). T1 VIBE FS was performed with the following parameters: repetition time/echo time (TR/TE), 4.06/1.89 ms; field of view (FOV), 380 mm; slice, 3 mm; flip angle, 10°; matrix, 340×274.

Image analysis

In the present study, three radiologists with more than 8 years of experience in abdominal MRI diagnosis assessed the data on the workstation (Version 4.0.0.9; Source, DJ HealthUnion Systems Corporation, Shanghai, China) of picture archiving and communication systems (PACS). Patients' personal and medical history information were concealed during the process.

Determination of HCPproposed and HCPEC

The HCP of initial IBD visualization from the dynamic HCPs were first determined independently by two

© Quantitative Imaging in Medicine and Surgery. All rights reserved.

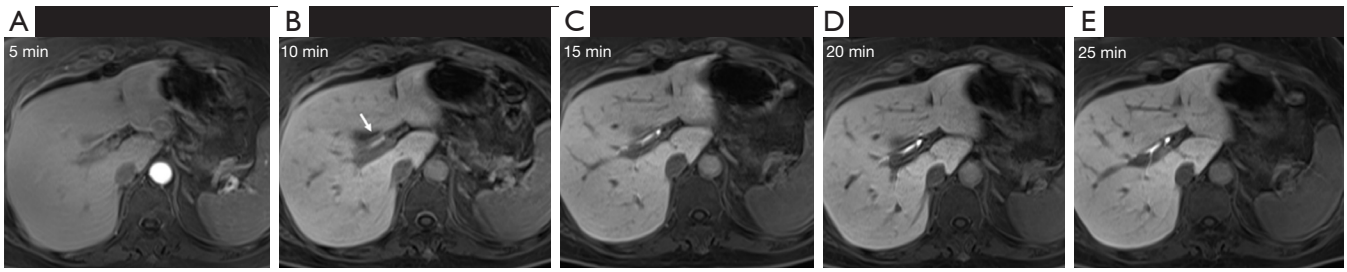

Figure 3 A female non-cirrhosis patient, 45 years old, 5 HCPs acquired with a time interval of 5 min from 5 to 25 min (A-E) after the Gd-EOB-DTPA administration. Two radiologists with 8 and 10 years of experience in abdominal MRI diagnosis both identified 10 min (B) as the initial intrahepatic bile duct visualization (white arrow) and so 15 min (C) as $HCP_{proposed}$. Two months later, the same 2 radiologists identified 15 min (C) and 20 min (D) as $HCP_{EC,}$ respectively, and the third radiologist arbitrated the HCP at 15 min as the HCP_{EC}. HCP, hepatocyte phase; Gd-EOB-DTPA, gadoxetic acid disodium; MRI, magnetic resonance imaging; $HCP_{proposed}$, the HCP acquired 5 min after the initial visualization of the intrahepatic bile ducts; HCP_{EC}, adequate HCP determined upon the 2016 Expert Consensus of the European Society of Gastrointestinal and Abdominal Radiology.

radiologists, each with 8 and 10 years of experience in abdominal MRI diagnosis, then the HCP acquired 5 min after the initial IBD visualization was recorded as the $HCP_{proposed}$, and the corresponding acquisition time after the administration of the GD-EOB-DTPA was recorded as the $Time_{proposed}$. Inconsistent results between the two radiologists were arbitrated by a third radiologist, who has 15 years of experience in abdominal MRI diagnosis. After 2 months, the two radiologists with 8 and 10 years of respective experience in abdominal MRI diagnosis independently determined from the dynamic HCPs the adequate HCP upon the 2016 EC of the ESGAR (16), namely, the HCP_{EC}, which was defined as when Gd-EOB-DTPA is detected in the IBDs and the vessels are definitely hypointense in comparison to the background parenchyma. The acquisition time correspondence to the HCP_{EC} was recorded as the $Time_{EC}$. Any inconsistent results between the two radiologists were arbitrated by the third radiologist (*Figures 3*,*4*).

Signal intensity measurement and parameters calculation

The signal intensity of the liver (SI_{liver}) was the mean of signal intensities of circular regions of interests (ROIs =100 mm²) in the left inner, left outer, right anterior, and right posterior lobes of the liver at the level of the porta hepatis. ROIs of the SI_{liver} were placed within the liver parenchyma at the same anatomic level on HCP_{EC} and $HCP_{proposed}$ images, carefully avoiding artifacts, lesions, vessels, and bile ducts. Hand-drawn ROIs adapting to the lesion contour were set for measurement of the signal intensity of the lesion (SI_{lesion}), in case of multiple hepatic lesions, the largest of which was chosen and assessed.

The above process was carried out independently by the two radiologists with 8 and 10 years of respective experience in abdominal MRI diagnosis. Their outcomes were averaged as the final results. The SI_{liver} was the average of the signal intensity of left lateral lobe (SI_{LLlobe}), left medial lobe (SI_{LMlobe}), right anterior lobe (SI_{RAlobe}), and right posterior lobe (SI_{RPlobe}). The SI_{liver}, hepatic relative enhancement ratio (RER), and lesions' contrast-to-noise ratio (CNR) and signal-to-noise ratio (SNR) were calculated by the following formulas:

$$\left(SI_{LMlobe} + SI_{LLlobe} + SI_{RAlobe} + SI_{RPlobe}\right) / 4 = SI_{liver} \quad [1]$$

$$\left(SI_{liverHCP} - SI_{liverpre\text{-}contrast}\right) / SI_{liverpre\text{-}contrast} = RER \quad [2]$$

$$\left(SI_{liver} - SI_{lesion}\right) / SD_{noise} = CNR \quad [3]$$

$$SI_{lesion} / SD_{noise} = SNR \quad [4]$$

SD_{noise} represented the standard deviation (SD) of the background noise in the phase-encoding direction.

Statistical analysis

The software SPSS 22.0 (IBM Corp., Armonk, NY, USA) was employed for data analysis. The Shapiro-Wilk test was performed for all the parameters to test normal distribution.

© Quantitative Imaging in Medicine and Surgery. All rights reserved.

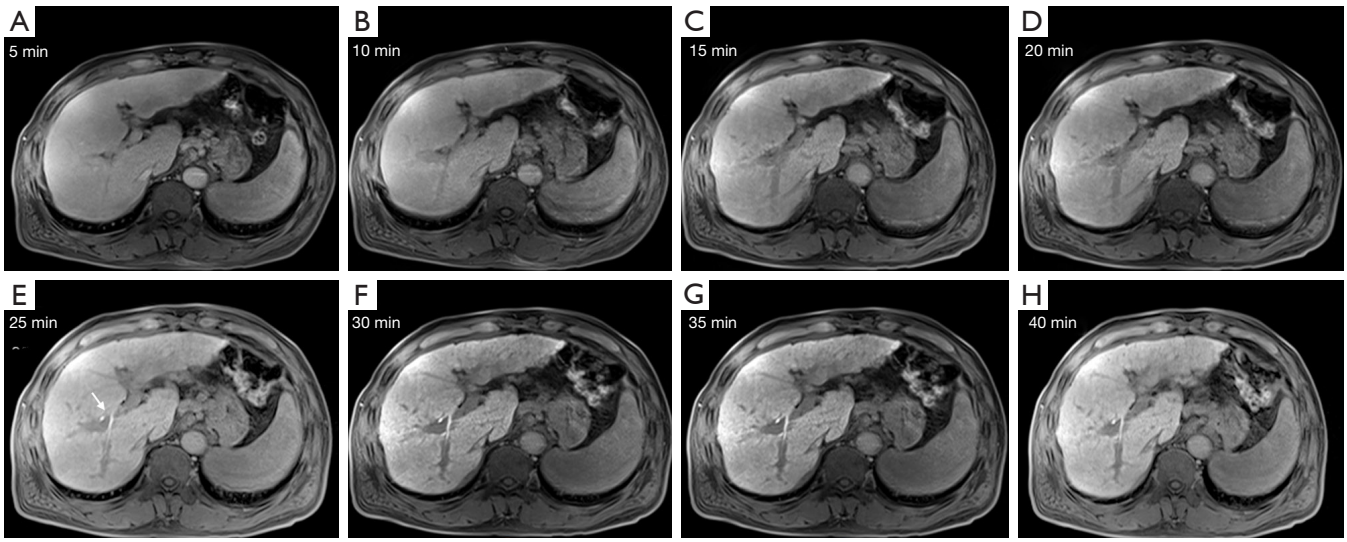

Figure 4 A male cirrhosis patient (CP B), 60 years old, with eight phases of the HCP imaged from 5 to 40 min (A-H) after the administration of the Gd-EOB-DTPA. Two radiologists with 8 and 10 years of experience in abdominal MRI diagnosis identified 25 min (E) as the initial intrahepatic bile duct visualization (white arrow) and so 30 min (F) as the $HCP_{proposed}$. Two months later, the same two radiologists identified 30 min (F) and 35 min (G) as the HCP_{EC}, respectively, then the third radiologist arbitrated the HCP at 35 min as the HCP_{EC}. CP, Child-Pugh; HCP, hepatocyte phase; Gd-EOB-DTPA, gadoxetic acid disodium; MRI, magnetic resonance imaging; $HCP_{proposed}$, the HCP acquired 5 min after the initial visualization of the intrahepatic bile ducts; HCP_{EC}, adequate HCP determined upon the 2016 Expert Consensus of the European Society of Gastrointestinal and Abdominal Radiology.

Parameters with the normal distribution were represented by mean ± SD. The paired *t*-test was performed to compare $Time_{EC}$ and $Time_{proposed}$ as well as RER, CNR, and SNR between the HCP_{EC} and $HCP_{proposed}$ for the $_{three}$ groups, respectively.

The reproducibility of the determination of the HCP_{EC} and $HCP_{proposed}$ was compared by the χ^2 test. Intraclass correlation coefficient (ICC) was used to assess the reproducibility of the measurements of the SI_{liver}, SI_{lesion}, and SD_{noise} between the two observers. The ICC values less than 0.5, between 0.5 and 0.75, between 0.75 and 0.9, and greater than 0.90 were indicative of poor, moderate, good, and excellent reproducibility, respectively (20). A two-sided P<0.05 was considered to indicate a significant difference.

Results

Ultimately, 107 patients were enrolled (65 males and 42 females) into this study (*Figure 1*), including 37 non-cirrhosis cases (51.3±14.76 years old; non-cirrhosis group) and 70 cirrhotic individuals (45, 20, 3, and 2 with hepatitis B, alcoholic, immune, and unknown-cause cirrhosis, respectively). In addition, none of the patients experienced adverse events after injection of the contrast agent. Totally, 101 non-cystic liver lesions with a diameter ≥1 cm were included in the analysis, with a median diameter of 2.30 cm (range, 1.2–9.1 cm) (*Table 1*).

Statistical comparisons of RER, CNR, and SNR between the HCPEC and HCPproposed

The RER, CNR, and SNR showed no significant differences between the HCP_{EC} and $HCP_{proposed}$ in non-cirrhosis group (P=0.20, P=0.67, and P=0.25), CP A group (P=0.09, P=0.16, and P=0.80), and CP B group (P=0.06, P=0.91, P=0.18), respectively (*Table 2*).

Time of the IBD initial visualization

Time of the IBD initial visualization ($Time_{IBD}$) was 10.00±1.67, 11.50±3.32, and 14.5±4.22 min in the three groups, respectively (*Figure 5*). In summary, a total of

© Quantitative Imaging in Medicine and Surgery. All rights reserved.

Table 1 The clinical information of all patients in the three groups.

Group	Number (M/F)	Age (years)	Hepatic focal lesions						
			HCCs	FNH	RNs	HCA	SNNs	HMC	HH
Non-cirrhosis	37 (20/17)	51.3±14.76	1	10	–	3	2	14	7
CP A	40 (28/12)	52.90±8.55	25	–	9	–	–	–	–
CP B	30 (17/13)	63.00±7.66	22	–	8	–	–	–	–
Total	107 (65/42)	–	48	10	17	3	2	14	7

Data are expressed as mean ± standard deviation or n. Number (M/F), the number of male and female patients; HCCs, hepatocellular carcinomas; FNH, focal nodular hyperplasia; RNs, regenerative nodules; HCA, hepatocellular adenoma; SNNs, solitary necrotic nodules; HMC, hepatic metastatic carcinomas; HH, hepatic hemangioma; CP, Child-Pugh.

Table 2 Statistical comparisons of RER, CNR and SNR between HCP_{EC} and $HCP_{proposed}$

Group	HCP	RER (n=107)		CNR (n=101)		SNR (n=101)	
		Mean ± SD	P value	Mean ± SD	P value	Mean ± SD	P value
Non-cirrhosis	$HCP_{proposed}$	1.16±0.37	0.20	189.60±67.39	0.67	169.60±88.99	0.25
	HCP_{EC}	1.17±0.36		191.50±68.32		172.00±89.03	
CP A	$HCP_{proposed}$	0.91±0.24	0.09	130.80±52.81	0.16	211.00±56.76	0.80
	HCP_{EC}	0.92±0.24		136.40±52.05		210.10±54.08	
CP B	$HCP_{proposed}$	0.74±0.35	0.06	133.25±8.23	0.91	175.40±63.79	0.18
	HCP_{EC}	0.75±0.34		133.44±8.51		173.20±64.50	

RER, relative enhancement ratio; CNR, contrast-to-noise ratio; SNR, signal-to-noise ratio; HCP_{EC}, adequate HCP determined upon the 2016 Expert Consensus of the European Society of Gastrointestinal and Abdominal Radiology; $HCP_{proposed}$, the HCP acquired 5 min after the initial visualization of the intrahepatic bile ducts; SD, standard deviation; HCP, hepatocyte phase; CP, Child-Pugh.

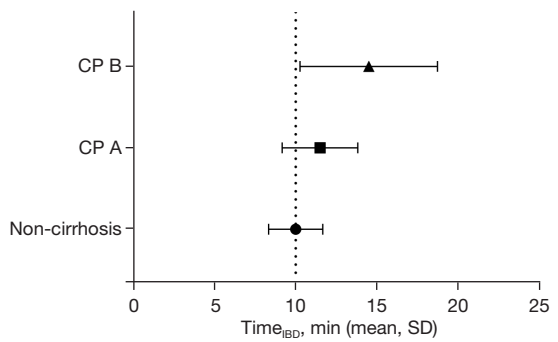

Figure 5 The forest plot of the $Time_{IBD}$ in three groups. CP, Child-Pugh; $Time_{IBD}$, time of the intrahepatic bile duct initial visualization; SD, standard deviation.

71 patients (66%) had $Time_{IBD}$ =10 min. More specifically, in the non-cirrhosis group (n=37), $Time_{IBD}$ was 5 min in 2 cases, 10 min in 33 (89%), and 15 min in 2; in the CP A group (n=40), time was 10 min in 28 cases (70%) and 15 min in 12; and in the CP B group (n=30), time was 10 min in 10 patients (33%), 15 min in 15, 20 min in 3, and 25 min in 2.

Statistical comparisons of TimeEC and Timeproposed

Paired differences between $Time_{EC}$ and $Time_{proposed}$ in the non-cirrhosis, CP A, and CP B groups were 1.08±3.56 min (P=0.07), 2.88±4.22 min (P<0.001), and 5.83±5.27 min

© Quantitative Imaging in Medicine and Surgery. All rights reserved.

Table 3 Statistical comparisons of $Time_{proposed}$ and $Time_{EC}$ in three groups

Group	HCP	Delay time (min), mean ± SD	Paired difference ($\bar{x}$±s), *t*, P value
Non-cirrhosis	$HCP_{proposed}$	15.00±1.67	(1.08±3.56), 1.85, 0.07
	HCP_{EC}	16.35±3.85	
CP A	$HCP_{proposed}$	16.50±3.32	(2.88±4.22), 4.31, <0.001
	HCP_{EC}	19.38±4.96	
CP B	$HCP_{proposed}$	19.50±4.22	(5.83±5.27), 6.07, <0.001
	HCP_{EC}	25.33±6.01	

$Time_{proposed}$, acquisition time of the $HCP_{propsoed}$ after the administration of the Gd-EOB-DTPA; $Time_{EC}$, acquisition time of the HCP_{EC} after the administration; HCP, hepatocyte phase; SD, standard deviation; CP, Child-Pugh; $HCP_{proposed}$, the HCP acquired 5 min after the initial visualization of the intrahepatic bile ducts; HCP_{EC}, adequate HCP determined upon the 2016 Expert Consensus of the European Society of Gastrointestinal and Abdominal Radiology.

(P<0.001), respectively (*Table 3*).

Inter-observer agreement

The MRI signal measurements of the two observers demonstrated good agreement. The ICCs were as follows: SI_{liver} [ICC =0.939; 95% confidence interval (CI): 0.932–0.945], SI_{lesion} (ICC =0.914; 95% CI: 0.885–0.936), and SD_{noise} (ICC =0.828; 95% CI: 0.773–0.870).

Inter-observer agreement of the determination of the HCP_{EC} and $HCP_{proposed}$ was 0.804 (86/107) and 0.962 (103/107), respectively, demonstrating a significant difference (χ^2=13.09, P=0.001).

Discussion

Although Gd-EOB-DTPA is considered the most efficient liver-specific MRI contrast agent in clinical practice, the relatively low speed of MRI scanning and delay acquisition of the HCP images result in a lengthy MRI examination of at least 30 min for Gd-EOB-DTPA-enhanced MRI (3,21,22). With the increasingly clinical application of Gd-EOB-DTPA-enhanced MRI, mounting attention is being paid to how to shorten the delay time of the HCP acquisition after intravenous administration while obtaining images with adequate diagnostic information. In this investigation, we found that the adequate HCP could be acquired 5 min after the initial visualization of the IBD, which could serve as a convenient and reproducible protocol for the HCP imaging.

Previous studies assessed the association of the delay time of the HCP acquisition with liver function, demonstrating that the better the liver function, the shorter the delay time required for adequate HCP acquisition (11-13). For the detection of liver lesions, patients with impaired liver function often need a longer time to increase the uptake of Gd-EOB-DTPA by liver parenchyma. Furthermore, recent studies have indicated that the timing of the initial visualization of the IBD is intrinsically associated with the liver function, the better the liver function, the earlier the initial visualization of the IBD after the administration (7,23). Consequently, the visualization of the IBD is utilized in optimizing the HCP acquisition protocol as one of the preconditions for consideration of an adequate HCP.

In the present study, 95% of the patients in the non-cirrhosis group (35/37) had the IBD visualized within 10 min after the administration of Gd-EOB-DTPA. Only 54.2% of cirrhotic patients (CP A + CP B) (38/70) had the IBD visualized within 10 min after the administration, which was slightly lower than that reported by Wu *et al.* (7) (65.4%). The reason may be that the proportion of CP A group patients in the cirrhotic patients (CP A + CP B) in our study is relatively lower than that in the study of Wu *et al.* (57.1% *vs.* 63.1%). In the present study, two patients in the non-cirrhosis group had the IBD visualized 5 min after the administration, which is consistent with the previous report (23), whereas the CP A and CP B groups had no IBD visualized in 5 min. The longest initial visualization of the IBD ($Time_{IBD}$) was 15 min (12/40) and 25 min (2/30) in the CP A and CP B groups, respectively. Wu *et al.* (7) reported that the $Time_{IBD}$ was postponed to 20 and 30 min in CP A patients and CP B/C patients, respectively.

In addition, Feng *et al.* (24) showed that the IBD in some cirrhotic patients did not visualize in 50 min after the Gd-EOB-DTPA administration, possibly because the genetic polymorphism in the OATP1B1 on the hepatocyte

© Quantitative Imaging in Medicine and Surgery. All rights reserved.

membrane affects the uptake rate of Gd-EOB-DTPA by hepatocytes (25). All patients in the present study had the IBD visualization within 40 min of the administration, possibly due to the non-inclusion of CP C patients or the limited sample size in our study.

Upon intravenous administration, Gd-EOB-DTPA is rapidly distributed in the intravascular space and then extravascular extracellular space with blood flow and perfusion. The signal of the liver parenchyma rises quickly within 2 to 3 min after the administration. Then, the parenchymal signal continues to rise, though relatively slowly, due to the hepatocytic uptake and intrahepatic accumulation of the Gd-EOB-DTPA. Subsequently, Gd-EOB-DTPA is excreted by multi-drug resistance protein 2 (MRP2) into bile ducts and exits the liver with the bile. The amount of the Gd-EOB-DTPA accumulated in the liver results from the dynamic balance between its uptake and excretion, and determines the SI_{liver} parenchyma. IBD visualization marks the beginning of Gd-EOB-DTPA excretion and suggests a consequent slowdown of the drug accumulation rate in the liver. Gradually, the Gd-EOB-DTPA uptake and excretion by the liver achieve a relative balance, resulting in a MR signal plateau of the hepatic parenchyma (8). Theoretically, the adequate HCP could be acquired in the whole stage of the MR signal plateau when the parenchymal signal remains at a high level and show good contrast to the intrahepatic lesion. The shortest delay time of the adequate HCP acquisition will be achieved at the initial stage of the MR signal plateau, which, however, is not reliably predictable. Based on the above analysis and the findings of the present study, we might predict that the initial stage of the hepatic MR signal plateau may occur at around 5 min after the IBD initial visualization. Previous research has suggested that the IBD initial visualization for patients with normal liver function is about 12 min (26). In addition, through observing the MRI signal intensity curves reported in several previous articles (8,27,28), we found that the initial stage of the MR signal plateau occurs at about 15–20 min after the Gd-EOB-DTPA administration. These findings strongly support our prediction.

The 2016 EC of the ESGAR provided two conditions for the consideration of the HCP as adequate: when Gd-EOB-DTPA is detected in the IBD and the vessels are definitely hypointense in comparison to the background parenchyma. Anatomically, the IBD includes the left and right hepatic ducts located in the hepatic hilum and their small intrahepatic branches at all levels. In patients without bile duct dilatation, the structures of the IBD that can be clearly identified in the Gd-EOB-DTPA-enhanced MRI are the left and right hepatic ducts and their major intrahepatic branches. Therefore, the judgement of the IBD visualization in the present study was confined to evaluation of the right and left hepatic ducts at the hepatic hilum level in the images of the HCP.

Additionally, the 2016 EC of the ESGAR does not provide any criteria for how to judge whether the vessels are definitely hypointense in comparison to the background parenchyma; it depends on the observer's personal experience. In the present study, to enhance the stability of our study findings, two senior diagnostic radiologists first assessed the images independently, and in case of disagreement, another senior diagnostic radiologist was involved to make final decision. The present study found an inter-observer agreement of 96% (103/107) for the $HCP_{proposed}$ determination, which was significantly higher than that of 80% (86/107) for the HCP_{EC} determination (χ^2=13.09, P<0.05). Such outcomes are mainly attributed to the subjectivity in the HCP_{EC} determination, namely, no objective criteria were provided on the judgement of "the vessels are definitely hypointense in comparison to the background parenchyma". In addition, the smaller SD values of $Time_{proposed}$ compared with $Time_{EC}$ also revealed the $HCP_{proposed}$ with upper precision and reliability compared with HCP_{EC} (*Table 3*), and this finding echoes the reproducibility of the determination of HCP.

A previous study investigated the use of the ratio of the liver signal intensity to that of the inferior vena cava (SIRLV) as an indicator to assess the adequacy of the HCP images in patients without chronic liver disease (CLD). This study concluded that if the SIRLV ≥2.0, the HCP is adequate and MR imaging could be stopped, thereby saving about 38% of the HCP acquisition waiting time in non-CLD patients (29). In addition, other investigators employed the liver-to-portal vein ratio (LPR) to assess the HCPs and demonstrated that the LPR ≥1.5 suggests an adequate HCP with improved lesions detection rate (30-32). Although the adequate HCP in these investigations is determined on objective criteria, it requires hand-draw ROIs and formular calculations by the operators during the MRI scanning, so might be of low operability. Furthermore, with the advent of artificial intelligence (AI) deep learning models, the convolutional neural networks were utilized to determine the adequacy of HCP for optimizing the HCP acquisition. It has been reported that the AI deep learning models may save approximately 48% of the HCP acquisition waiting time in cirrhotic patients (33). However, its generalizability and

© Quantitative Imaging in Medicine and Surgery. All rights reserved.

robustness need to be validated, and its clinical application faces great challenges (34,35).

This study has several limitations. First, patients with severe hepatic impairment (CP C) were not included, which may make our findings inapplicable to such patients. Second, considering the total MRI examination time, patient compliance and the MRI protocol's operability, the time interval for dynamic HCP image acquisition was set at 5 min, although it would have been further reduced to increase the temporal resolution of the HCP sampling. A smaller acquisition time interval, for example, a 2- or 3-min interval, may produce more accurate findings. Third, the proposed protocol for the HCP acquisition in Gd-EOB-DTPA-enhanced MRI are not applicable to patients without the IBD visualization, which were not encountered in the present study, mainly because of non-inclusion of patients with severe hepatic impairment and biliary obstruction, or a limited sample size.

Conclusions

The adequate HCP could be acquired 5 min after the initial visualization of the IBD. We developed a convenient and reproducible protocol for adequate HCP acquisition in Gd-EOB-DTPA-enhanced MRI. This protocol enables radiologists to quickly determine reasonable HCP delay times and efficiently perform Gd-EOB-DTPA-enhanced MRI scan, especially for liver function impaired patients.

Acknowledgments

Funding: This work was support by the National Natural Science Foundation of China (81671680).

Footnote

Reporting Checklist: The authors have completed the STROBE reporting checklist. Available at https://qims.amegroups.com/article/view/10.21037/qims-23-1147/rc

Conflicts of Interest: All authors have completed the ICMJE uniform disclosure form (available at https://qims.amegroups.com/article/view/10.21037/qims-23-1147/coif). The authors have no conflicts of interest to declare.

Ethical Statement: The authors are accountable for all aspects of the work in ensuring that questions related to the accuracy or integrity of any part of the work are appropriately investigated and resolved. The study was conducted in accordance with the Declaration of Helsinki (as revised in 2013). The study was approved by institutional ethics board of the 8th Medical Center of PLA General Hospital (30920200825701240) and informed consent was taken from all individual participants.

Open Access Statement: This is an Open Access article distributed in accordance with the Creative Commons Attribution-NonCommercial-NoDerivs 4.0 International License (CC BY-NC-ND 4.0), which permits the non-commercial replication and distribution of the article with the strict proviso that no changes or edits are made and the original work is properly cited (including links to both the formal publication through the relevant DOI and the license). See: https://creativecommons.org/licenses/by-nc-nd/4.0/.

References

1. Hamm B, Staks T, Mühler A, Bollow M, Taupitz M, Frenzel T, Wolf KJ, Weinmann HJ, Lange L. Phase I clinical evaluation of Gd-EOB-DTPA as a hepatobiliary MR contrast agent: safety, pharmacokinetics, and MR imaging. Radiology 1995;195:785-92.
2. Cruite I, Schroeder M, Merkle EM, Sirlin CB. Gadoxetate disodium-enhanced MRI of the liver: part 2, protocol optimization and lesion appearance in the cirrhotic liver. AJR Am J Roentgenol 2010;195:29-41.
3. Ringe KI, Husarik DB, Sirlin CB, Merkle EM. Gadoxetate disodium-enhanced MRI of the liver: part 1, protocol optimization and lesion appearance in the noncirrhotic liver. AJR Am J Roentgenol 2010;195:13-28.
4. Haimerl M, Verloh N, Zeman F, Fellner C, Nickel D, Lang SA, Teufel A, Stroszczynski C, Wiggermann P. Gd-EOB-DTPA-enhanced MRI for evaluation of liver function: Comparison between signal-intensity-based indices and T1 relaxometry. Sci Rep 2017;7:43347.
5. Guimaraes L, Babaei Jandaghi A, Menezes R, Grant D, Cattral M, Jhaveri KS. Assessment of biliary anatomy in potential living liver donors: Added value of gadoxetic acid-enhanced T1 MR Cholangiography (MRC) including utilization of controlled aliasing in parallel imaging results in higher acceleration (CAIPIRINHA) technique in comparison to T2W-MRC. Magn Reson Imaging 2020;70:64-72.
6. Hayoz R, Vietti-Violi N, Duran R, Knebel JF, Ledoux JB, Dromain C. The combination of hepatobiliary phase with Gd-EOB-DTPA and DWI is highly accurate for the

© Quantitative Imaging in Medicine and Surgery. All rights reserved.

detection and characterization of liver metastases from neuroendocrine tumor. Eur Radiol 2020;30:6593-602.
7. Wu J, Li H, Lin Y, Chen Z, Zhong Q, Gao H, Fu L, Sandrasegaran K. Value of gadoxetate biliary transit time in determining hepatocyte function. Abdom Imaging 2015;40:95-101.
8. Akimoto S, Mori H, Fujii T, Furuya K. Optimal scan timing for Gd-EOB-DTPA enhanced liver dynamic MR imaging. Nihon Hoshasen Gijutsu Gakkai Zasshi 2009;65:626-30.
9. Motosugi U, Ichikawa T, Tominaga L, Sou H, Sano K, Ichikawa S, Araki T. Delay before the hepatocyte phase of Gd-EOB-DTPA-enhanced MR imaging: is it possible to shorten the examination time? Eur Radiol 2009;19:2623-9.
10. Jeong HT, Kim MJ, Park MS, Choi JY, Choi JS, Kim KS, Choi GH, Shin SJ. Detection of liver metastases using gadoxetic-enhanced dynamic and 10- and 20-minute delayed phase MR imaging. J Magn Reson Imaging 2012;35:635-43.
11. van Kessel CS, Veldhuis WB, van den Bosch MA, van Leeuwen MS. MR liver imaging with Gd-EOB-DTPA: a delay time of 10 minutes is sufficient for lesion characterisation. Eur Radiol 2012;22:2153-60.
12. Liang M, Zhao J, Xie B, Li C, Yin X, Cheng L, Wang J, Zhang L. MR liver imaging with Gd-EOB-DTPA: The need for different delay times of the hepatobiliary phase in patients with different liver function. Eur J Radiol 2016;85:546-52.
13. Wu JW, Yu YC, Qu XL, Zhang Y, Gao H. Optimization of hepatobiliary phase delay time of Gd-EOB-DTPA-enhanced magnetic resonance imaging for identification of hepatocellular carcinoma in patients with cirrhosis of different degrees of severity. World J Gastroenterol 2018;24:415-23.
14. Rao SX, Wang J, Wang J, Jiang XQ, Long LL, Li ZP, Li ZL, Shen W, Zhao XM, Hu DY, Zhang HM, Zhang L, Huan Y, Liang CH, Song B, Zeng MS. Chinese consensus on the clinical application of hepatobiliary magnetic resonance imaging contrast agent: Gadoxetic acid disodium. J Dig Dis 2019;20:54-61.
15. Esterson YB, Flusberg M, Oh S, Mazzariol F, Rozenblit AM, Chernyak V. Improved parenchymal liver enhancement with extended delay on Gd-EOB-DTPA-enhanced MRI in patients with parenchymal liver disease: associated clinical and imaging factors. Clin Radiol 2015;70:723-9.
16. Neri E, Bali MA, Ba-Ssalamah A, Boraschi P, Brancatelli G, Alves FC, Grazioli L, Helmberger T, Lee JM, Manfredi R, Martì-Bonmatì L, Matos C, Merkle EM, Op De Beeck B, Schima W, Skehan S, Vilgrain V, Zech C, Bartolozzi C. ESGAR consensus statement on liver MR imaging and clinical use of liver-specific contrast agents. Eur Radiol 2016;26:921-31.
17. Tsoris A, Marlar CA. Use Of The Child Pugh Score In Liver Disease. 2023 Mar 13. In: StatPearls [Internet]. Treasure Island (FL): StatPearls Publishing; 2023.
18. LI-RADS® v2018 Core [Internet]. American College of Radiology; v2018 [cited 2022 April 2]. Available online: https://www.acr.org/Clinical-Resources/Reporting-and-Data-Systems/LI-RADS
19. Zech CJ, Ba-Ssalamah A, Berg T, Chandarana H, Chau GY, Grazioli L, Kim MJ, Lee JM, Merkle EM, Murakami T, Ricke J, B Sirlin C, Song B, Taouli B, Yoshimitsu K, Koh DM. Consensus report from the 8th International Forum for Liver Magnetic Resonance Imaging. Eur Radiol 2020;30:370-82.
20. Koo TK, Li MY. A Guideline of Selecting and Reporting Intraclass Correlation Coefficients for Reliability Research. J Chiropr Med 2016;15:155-63.
21. Kim YK, Kim CS, Han YM, Park G. Detection of small hepatocellular carcinoma: can gadoxetic acid-enhanced magnetic resonance imaging replace combining gadopentetate dimeglumine-enhanced and superparamagnetic iron oxide-enhanced magnetic resonance imaging? Invest Radiol 2010;45:740-6.
22. Park G, Kim YK, Kim CS, Yu HC, Hwang SB. Diagnostic efficacy of gadoxetic acid-enhanced MRI in the detection of hepatocellular carcinomas: comparison with gadopentetate dimeglumine. Br J Radiol 2010;83:1010-6.
23. Bollow M, Taupitz M, Hamm B, Staks T, Wolf KJ, Weinmann HJ. Gadolinium-ethoxybenzyl-DTPA as a hepatobiliary contrast agent for use in MR cholangiography: results of an in vivo phase-I clinical evaluation. Eur Radiol 1997;7:126-32.
24. Feng ST, Wu L, Chan T, Cai H, Luo Y, Zheng K, Tang D, Li ZP. Functional magnetic resonance cholangiography enhanced with Gd-EOB-DTPA: effect of liver function on biliary system visualization. J Magn Reson Imaging 2014;39:1254-8.
25. Nassif A, Jia J, Keiser M, Oswald S, Modess C, Nagel S, Weitschies W, Hosten N, Siegmund W, Kühn JP. Visualization of hepatic uptake transporter function in healthy subjects by using gadoxetic acid-enhanced MR imaging. Radiology 2012;264:741-50.
26. Ringe KI, Husarik DB, Gupta RT, Boll DT, Merkle EM. Hepatobiliary transit times of gadoxetate disodium

© Quantitative Imaging in Medicine and Surgery. All rights reserved.

(Primovist®) for protocol optimization of comprehensive MR imaging of the biliary system--what is normal? Eur J Radiol 2011;79:201-5.
27. Brismar TB, Dahlstrom N, Edsborg N, Persson A, Smedby O, Albiin N. Liver vessel enhancement by Gd-BOPTA and Gd-EOB-DTPA: a comparison in healthy volunteers. Acta Radiol 2009;50:709-15.
28. Sirlin CB, Hussain HK, Jonas E, Kanematsu M, Min Lee J, Merkle EM, Peck-Radosavljevic M, Reeder SB, Ricke J, Sakamoto M. Consensus report from the 6th International forum for liver MRI using gadoxetic acid. J Magn Reson Imaging 2014;40:516-29.
29. Bashir MR, Breault SR, Braun R, Do RK, Nelson RC, Reeder SB. Optimal timing and diagnostic adequacy of hepatocyte phase imaging with gadoxetate-enhanced liver MRI. Acad Radiol 2014;21:726-32.
30. Takatsu Y, Nakamura M, Kobayashi S, Miyati T. Visual criterion for evaluating hepatobiliary phase image acquisition of gadolinium-ethoxybenzyl-diethylenetriaminepentaacetic acid-enhanced MRI. Clin Radiol 2018;73:760.e1-6.
31. Takatsu Y, Nakamura M, Shiozaki T, Narukami S, Yoshimaru D, Miyati T, Kobayashi S. Assessment of the cut-off value of quantitative liver-portal vein contrast ratio in the hepatobiliary phase of liver MRI. Clin Radiol 2021;76:551.e17-24.
32. Mori Y, Motosugi U, Shimizu T, Ichikawa S, Kromrey ML, Onishi H. Predicting Patients With Insufficient Liver Enhancement in the Hepatobiliary Phase Before the Injection of Gadoxetic Acid: A Practical Approach Using the Bayesian Method. J Magn Reson Imaging 2020;51:62-9.
33. Cunha GM, Hasenstab KA, Higaki A, Wang K, Delgado T, Brunsing RL, Schlein A, Schwartzman A, Hsiao A, Sirlin CB, Fowler KJ. Convolutional neural network-automated hepatobiliary phase adequacy evaluation may optimize examination time. Eur J Radiol 2020;124:108837.
34. Chan HP, Samala RK, Hadjiiski LM, Zhou C. Deep Learning in Medical Image Analysis. Adv Exp Med Biol 2020;1213:3-21.
35. Sanaat A, Shiri I, Ferdowsi S, Arabi H, Zaidi H. Robust-Deep: A Method for Increasing Brain Imaging Datasets to Improve Deep Learning Models' Performance and Robustness. J Digit Imaging 2022;35:469-81.

Cite this article as: Wang C, Sun WR, Wu N, Zhang Z, Zhang LX, Yi WQ, Yuan XD. A convenient and reproducible protocol for acquisition of the hepatocyte phase for liver function-impaired patients in gadoxetic acid disodium-enhanced magnetic resonance imaging. Quant Imaging Med Surg 2024;14(2):1904-1915. doi: 10.21037/qims-23-1147

© Quantitative Imaging in Medicine and Surgery. All rights reserved.